The Oxygen Transport Efficiency of Arthropod Hemocyanins

Authors: Kobayashi, Michiyori, Kitayama, Kazuko, Watanabe, Miho, and Makino, Nobuo

Source: Zoological Science, 12(3) : 271-276

Published By: Zoological Society of Japan

URL: https://doi.org/10.2108/zsj.12.271

ZOOLOGICAL SCIENCE 12: 271–276 (1995)

The Oxygen Transport Efficiency of Arthropod Hemocyanins

MICHIYORI KOBAYASHI*, KAZUKO KITAYAMA, MIHO WATANABE
and NOBUO MAKINO**

Department of Biology, Faculty of Science, Niigata University, Niigata 950-21, and [1]Institute of Basic Medical Science, University of Tsukuba, Tsukuba, Ibaraki 305, Japan

ABSTRACT—The efficiency in O_2 transport of an O_2 carrier is best expressed by the slope of O_2 equilibrium curve (dS/dP), where S and P denote the fractional O_2 saturation of the carrier and the partial O_2 pressure, respectively. The aim of this study is to characterize the O_2 binding to arthropod hemocyanins (Hcs) in term of the O_2 transport efficiency, and for that purpose we have reexamined the previously published O_2 equilibrium data and their mathematical interpretations. Examination of the data for 6- and 12-meric Hcs from lobsters (*Panulirus japonicus, Procambarus clarkii*) revealed the relationship $P_{dmax} < P_{50} \approx P_{nmax}$, where P_{dmax}, P_{50} and P_{nmax} denote the P at which dS/dP is maximized, P at half-saturation and P at which the Hill coefficient is maximized, respectively. On the other hand, 48-meric Hcs from horseshoe crabs (*Tachypleus gigas*, and *Limulus polyphemus*) gave the relationship $P_{dmax} \leq P_{50} < P_{nmax}$, when the O_2 binding is cooperative. The results indicate that Hc functions most effectively at P values lower than that expected from the maximal degree of cooperativity, similarly to the previous results obtained for human hemoglobin (Hb) [6]. The profile of dS/dP *vs.* P curves for lobster Hcs was similar to that of Hb, showing a single maximum and a relatively symmetric shape. On the other hand, the curves for horseshoe crab Hcs showed multiple maxima tailing in the low P range, indicating that the O_2 transport efficiency is high even under hypoxic circumstances. As far as the O_2 transport efficiency is concerned, horseshoe crab Hcs are regarded as unique, and the features seem to reflect their uniqueness in the molecular architecture and the mode of allosteric transition.

INTRODUCTION

Hemocyanin (Hc) is a copper-containing O_2 carrier found in the hemolymph of many arthropods and mollusks. In arthropod Hcs, molecular mass of the subunit is about 75 kDa, and the whole molecules are composed of 6, 12, 24 or 48 subunits. The 6-meric unit is regarded as the "binding block", and the size of the molecule is controlled by the "linker" subunits, which bridge between the structural units. Under the physiological conditions they show cooperativity in the O_2 binding, which enables efficient loading and unloading of O_2. Their O_2 equilibria have been described on the basis of allosteric model of Monod *et al.*[13], but various extensions of the model have been introduced to describe them systematically [1, 3, 7, 14, 15]. Although the cooperativity of Hc has often been discussed in analogy to that of Hb, they have several different features, which presumably arise from their different molecular architectures and subunit interactions.

The magnitude of cooperativity in an O_2 carrier has usually been discussed in terms of the slope of the Hill plot (n), but the efficiency of O_2 transport is best expressed by the slope of O_2 equilibrium curve, dS/dP (S'), where S and P stand for the O_2 saturation of the O_2 carrier and the partial pressure of O_2, respectively. The quantity, S', directly relates to the amount of O_2 loaded or unloaded on a small change in P. Figure 1 shows the S *vs.* P and S' *vs.* P curves for cooperative (Hb) and non-cooperative (Mb) O_2 binding. The curves for Hb were obtained from the experimentally obtained Adair constants [5]. The curves for the non-cooperative binding (such as the binding to Mb) were calculated numerically on the assumption of the hyperbolic binding function. The S' *vs.* P curve for Hb is characterized by a relatively symmetric shape with a single maximum, while the non-cooperative binding is characterized by a monotonously decreasing curve without any maximum. Our preceding study [6] showed that in human Hb the relation $P_{dmax} < P_{50} <$

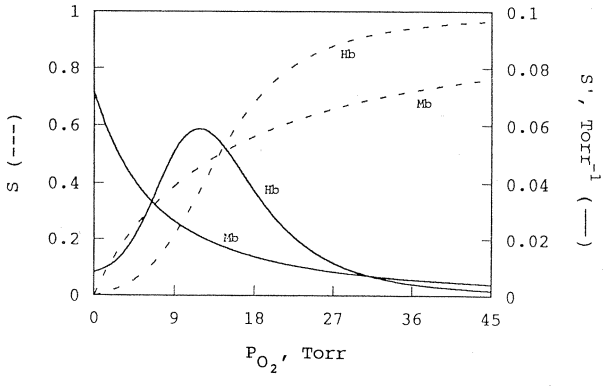

FIG. 1. O_2 equilibrium and transport efficiency of human Hb and a non-cooperative carrier. Hb at pH 7.4, 0.1 M Cl^-, 2 mM DPG (P_{50}=14.0 Torr), calculated from the Adair constants [5]. Non-cooperative O_2 binding, calculated for P_{50}=14.0 Torr. The dashed and solid lines show the S *vs.* P and S' *vs.* P curves, respectively.

Accepted March 24, 1995
Received December 19, 1994
* To whom all correspondence should be addressed.
** Present address, Ibaraki Prefectural University of Health Science, Ami, Ibaraki 300-03, Japan

P_{nmax} holds generally, where P_{dmax}, P_{50} and P_{nmax} are P at which S' is maximized, P at the half-saturation and P at which n is maximized, respectively. The result indicates that Hb transports O_2 most effectively at P lower than that expected from the maximal degree of cooperativity. In Hb the S value giving the maximum S' (S'_{max}) was about 0.38 irrespectively of the experimental conditions.

The aim of this study is to examine the O_2 transport efficiency of arthropod Hcs in comparison with that of Hb. We have reexamined the O_2 equilibrium data and cooperativity models previously presented for Hcs of two Decapoda species (spiny lobster *Panulirus japonicus* and crayfish *Procambarus clarkii*) and two Xiphosura species (horseshoe crabs, *Tachypleus gigas* and *Limulus polyphemus*). *Panulirus* has 6-meric Hc, while *Procambarus* contains 6-meric and 12-meric Hc molecules that are not interchangeable [10]. The horseshoe crab Hcs are 48-meric and are characterized by high Hill coefficients ($n=3$ to 5) [3]. In this study we have found distinct differences in the O_2 transport efficiency profile between the lobster and horseshoe crab Hcs, which seems to reflect the differences in the mechanism of the allosteric transitions.

MATERIALS AND METHODS

For the calculation of ΔS *vs.* P plots we have used previously published O_2 equilibrium data for Hcs of *Panulirus japonicus* (spiny lobster)[7], *Procambarus clarkii* (crayfish) [10] and *Tachypleus gigas* (horseshoe crab) [8]. The O_2 equilibrium data were smoothed by a moving average method. Then the change in S was calculated from the smoothed data and expressed as ΔS per 1 Torr. In addition, we also calculated the theoretical S' *vs.* P curves on the basis of the fitted mathematical models. In the preceding paper [6] on Hb, we have calculated the O_2 transport efficiency on the basis of Adair equation. In Hc, however, the order of the equation is too high (6 or more), and it is generally difficult to obtain a statistically significant set of values for the Adair constants. We therefore decided to apply the previously published results of model fitting studies. For arthropod Hcs a considerable number of theoretical studies have been published, but for the present purpose it is important whether the mathematical model can reproduce the O_2 equilibrium of the Hc in question with a sufficient accuracy, rather than whether it is theoretically valid. On this criterion we selected the following O_2 binding model and calculated the S' *vs.* P plots, as described below, using the reported parameter values. The used models were :the three-state model for *Panulirus* Hc [7], the two-state model for *Procambarus* and *Tachypleus* Hcs [8, 10] and the "interacting cooperative unit (ICU)" model for *Limulus* Hc [3].

According to the theory of Wyman [18] S is calculated from the binding polynomial B as:

$$S=(1/m)(P/B)(dB/dP) \tag{1}$$

where m is the number of interacting subunits. The function B depends on the mathematical model. From Eq.(1), S' is given as

$$S'=(1/m)\{(P/B)(d^2B/dP^2)+(dB/dP)[B-P(dB/dP)]/B^2\} \tag{2}$$

and S'_0 (S' at $P=0$) is obtained as

$$S'_0=(1/m)(dB/dP)(1/B) \tag{3}$$

The S'_0 value corresponds to the affinity of the carrier for the first ligand (O_2) molecule.

In the original model of Monod *et al.* [13] an allosteric equilibrium was assumed between two different affinity states (R and T), but the model was extended to three affinity states by Minton and Imai [12] to apply to the O_2 binding to Hb. The binding polynomial for the two-state model is written as

$$B(\text{two-state})=[(1+K_RP)^m+L(1+K_TP)^m]/(1+L) \tag{4}$$

and S'_0 is calculated as

$$S'_0(\text{two-state})=(K_R+K_TL)/(1+L) \tag{5}$$

For the three-state model,

$$B(\text{three-state})=[(1+K_RP)^m+M(1+K_SP)^m+L(1+K_TP)^m]/(1+M+L) \tag{6}$$

and

$$S'_0(\text{three-state})=(K_R+K_SM+K_TL)/(1+M+L) \tag{7}$$

where K_R, K_T and K_S are the O_2 equilibrium constants for the states R, T and S, respectively. L and M are the allosteric equilibrium constants ([T]/[R] and [S]/[R], respectively). It should be noted that all the four parameters (m, L, K_R and K_T) in Eq. (4) must be variable when the two-state model was applied to the O_2 binding to *Procambarus* and *Tachypleus* Hcs [8, 10].

Brouwer and Serigstad [3] proposed the "interacting cooperative unit (ICU)" model to describe the O_2 equilibrium of *Limulus* Hc. In this model an equilibrium is assumed between the functional m-mer and 2m-mer, in each of which an additional equilibrium is assumed to exist between the states R and T. The binding polynomial is written as

$$B(\text{ICU})=[(1+K_RP)^m+L(1+K_TP)^m+2I(1+K'_RP)^{2m}+2L_1I(1+K'_TP)^{2m}]/(1+L+2I+2L_1I) \tag{8}$$

and

$$S'_0=(K_R+LK_T+4IK'_R+4L_1IK'_T)/(1+L+2I+2L_1I) \tag{9}$$

where K'_R and K'_T are the O_2 association constants for the cooperative units composed of $2m$ subunits in the states R and T, respectively. The equilibrium constants, L, I, and L_1, are defined as $[T_m]/[R_m]$, $[R_{2m}]/[R_m]$, and $[T_{2m}]/[R_{2m}]$, respectively.

The numerical calculation was performed with programs compiled with MS-FORTRAN on an NEC 9801 model DA personal computer.

RESULTS

Figure 2A and 2B show the S *vs.* P and ΔS *vs.* P plots calculated from the O_2 equilibrium data for *Panulirus* Hc and *Procambarus* 12-mer Hc [7, 10]. The ΔS *vs.* P plots for the lobster Hcs showed a single maximum and a relatively symmetric shape, which closely resemble those for human Hb (Fig. 1). In *Procambarus* Hc, the n values for the 6-mer were somewhat lower than those for the 12-mer [10], but no substantial difference was observed in the profile of S' *vs.* P plots (data not shown).

Figure 2C shows the S *vs.* P and ΔS *vs.* P plots for

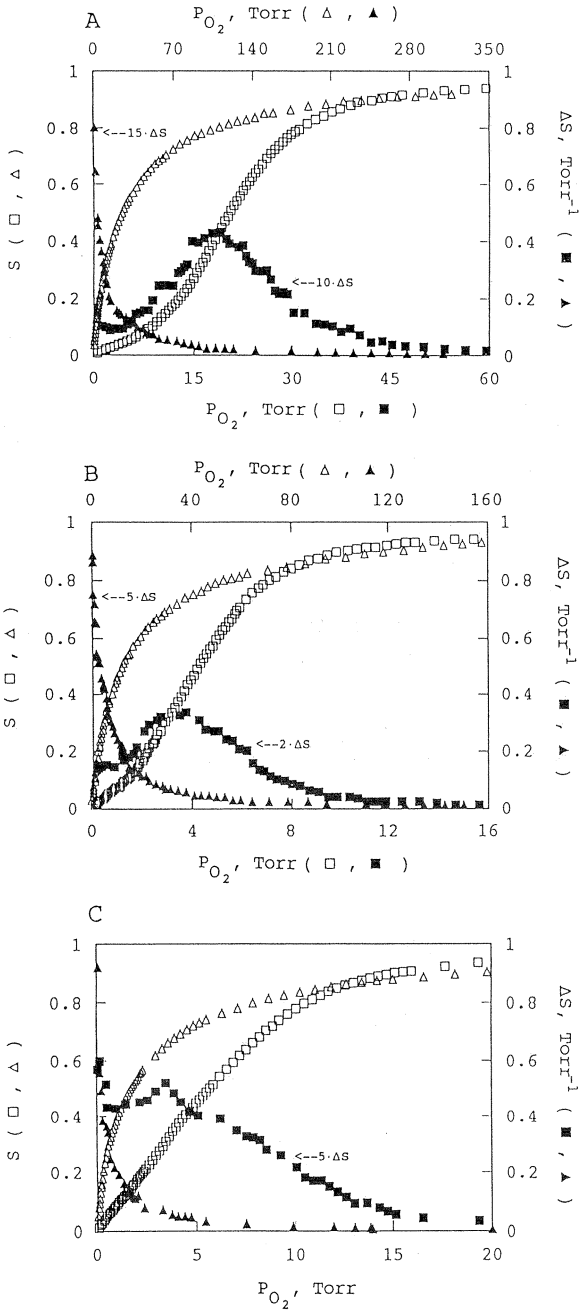

FIG. 2. O_2 equilibrium and ΔS *vs.* P plot of decapod Hcs. The open and closed symbols show the O_2 equilibrium and ΔS vs. P plots, respectively. (A) *Panulirus* Hc [7]. (square) Cooperative O_2 binding at pH 7.5 in the presence of 10 mM $CaCl_2$ (P_{50}=20.6 Torr). (triangle) Non-cooperative O_2 binding to EDTA-treated Hc at pH 9.5 (P_{50}=17.6 Torr). (B) *Procambarus* Hc 12-mer [10]. (square) Cooperative O_2 binding in physiological saline at pH 7.5 (P_{50}=4.33 Torr). (triangle) Non-cooperative O_2 binding at pH 9.5 in the presence of 1 mM EDTA (P_{50}=12.49 Torr). (C) *Tachypleus* Hc [8]. (square) Cooperative O_2 binding in physiological saline at pH 7.33 (P_{50}=5.54 Torr). (triangle) Non-cooperative O_2 binding at pH 9.03 in the presence of 1 mM EDTA (P_{50}=1.47 Torr).

Tachypleus Hc obtained from the O_2 equilibrium data. Under the physiological conditions, however, its ΔS *vs.* P plot was considerably different from those for the lobster Hcs and human Hb described above. Its shape was broader and asymmetric, spreading to the lower P range.

When Hcs from three species dissociated into the subunits by treatment with EDTA, it shows a hyperbolic O_2 binding curve characteristic of the non-cooperative ligand binding as shown in Figure 1.

Figure 3A shows the S *vs.* P and S' *vs.* P curves for *Panulirus* and *Procambarus* Hcs which were obtained mathe-

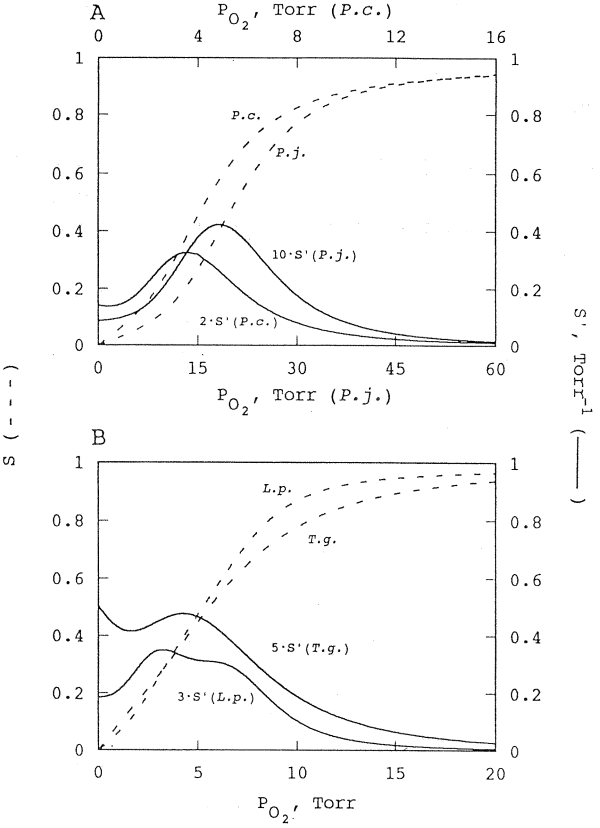

FIG. 3. O_2 equilibrium and transport efficiency of Hcs calculated on the basis of the cooperativity models. The dashed and solid lines show the S *vs.* P and S' *vs.* P curves, respectively. (A) (*P.j.*) S and S' for *Panulirus* Hc, calculated on the basis of the three-state model with the parameter values fitted to the O_2 equilibrium data shown in Fig. 2A (m=6, L=2.97×10^6, M=2.99×10^4, K_T=0.008 Torr^{-1}, K_R=0.6 Torr^{-1}, and K_S=0.0624 Torr^{-1}) [7]. (*P.c.*) S and S' for *Procambarus* Hc 12-mer, calculated on the basis of the two-state model with the parameter values fitted to the O_2 equilibrium data shown in Fig. 2B (m=5.22, L=6.53×10^3, K_T=0.0702 Torr^{-1}, and K_R=1.32 Torr^{-1}) [10]. Scales of abscissa, for *Procambarus* (top) and *Panulirus* (bottom) Hcs. (B) (*T.g.*) S and S' for *Tachypleus* Hc, calculated on the basis of the two-state model with the parameter values fitted to the O_2 equilibrium data shown in Fig. 2C (m=4.61, L=1.81×10^7, K_T=0.101 Torr^{-1} and K_R=7.94 Torr^{-1}) [8]. (*L.p.*) S and S' for *Limulus* Hc, calculated on the ICU model with the parameter values fitted to the O_2 equilibrium data at pH 7.4 in the presence of 10 mM Ca^{2+} (L=1.546×10^3, L_1=6.418×10^9, I=3.972×10^{-7}, K_T=16.08 Torr$_{-1}$, K'_T=7.23 Torr$_{-1}$, K_R=K'_R=0.61 Torr$_{-1}$) [3].

matically on the basis of cooperativity models. The *S' vs. P* curves for *Panulirus* Hc were computed on the three-state model with the parameter values fitted to the data shown in Figure 2A [7]. The *S' vs. P* curves for *Procambarus* Hc were obtained on the basis of the two-state model with the four variable parameters (*m, L,* K_R and K_T) [10]; the parameter values fitted to the data shown in Figure 2B were used for the computation. As expected from the goodness of the fit, the calculated *S'* curves well reproduced the observation (Fig. 2A and 2B).

Figure 3B shows the *S vs. P* and *S' vs. P* curves for *Tachypleus* and *Limulus* Hcs. The *S' vs. P* curve for *Tachypleus* Hc was obtained on the basis of the two-state model with four parameter values fitted to the data shown in Figure 2C [8], and it showed a good agreement with the observed data. The curve for *Limulus* Hc was computed according to the ICU model together with fitted parameter values that were presented by Brouwer and Serigstad [3]. Similarly to the results on *Tachypleus* Hc, the *S' vs. P* curve for *Limulus* Hc was characterized by multiple peaks and rather an asymmetric shape.

Figure 4 shows the P_{dmax} and P_{nmax} values as a function of P_{50} under various conditions where the Hcs show the cooperativity in O_2 binding. The data points were obtained mathematically on the basis of the cooperative models using fitted parameter values, as described in Methods. As judged from the goodness of the models, the error arising from the model fitting is estimated to be small and thus negligible. In *Panulirus* and *Procambarus* Hcs, as shown in Figure 4A, the P_{nmax} value was generally close to the P_{50} value, but both values were significantly greater than the corresponding P_{dmax} value. In the horseshoe crab Hcs, on the other hand, the P_{dmax} values were nearly equal to or smaller than the corresponding P_{50} values, while the P_{nmax} values were considerably greater than the P_{50} values (Fig. 4B). In this respect, horseshoe Hcs were also different from the vertebrate Hb and lobster Hcs.

Figure 5 shows the maximum $S'(S'_{max})$ values and *S'* values at $P=0$ (S'_0) as functions of P_{dmax} for Hb and Hcs under the conditions where they bind O_2 cooperatively. The plot for *Panulirus* Hc (and *Procambarus* Hc, though data are not shown) was very similar to that for Hb; both S'_{max} and S'_0 changed greatly with the change in P_{dmax} (and consequently with P_{50}). *Limulus* Hc was also unique on this point, and S'_{max} was almost constant in spite of the wide variation of P_{dmax} (Fig. 5A). As seen in figure 5B, the S'_0 for *Limulus* Hc was independent of P_{dmax}, though the plot was more scattered. In *Tachypleus* Hc, the significant difference was

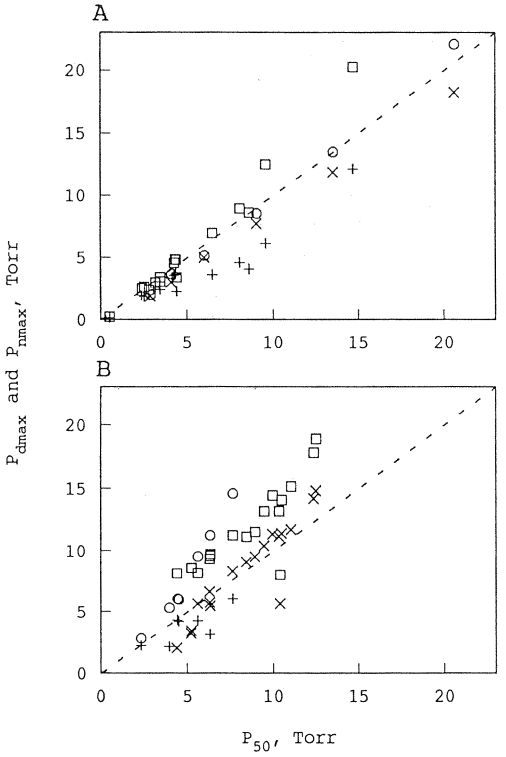

FIG. 4. Relationship between P_{dmax}, P_{nmax} and P_{50} in the cooperative O_2 binding to Hcs. Open symbols, P_{nmax}; cross and plus symbols, P_{dmax}. (A) Lobster Hcs. (circle and cross) *Panulirus* Hc, (square and plus) *Procambarus* Hc 12-mer and 6-mer. (B) Horseshoe crab Hcs. (circle and plus) *Tachypleus* Hc, (square and cross) *Limulus* Hc. The values for P_{dmax}, P_{nmax} and P_{50} were obtained from the mathematical models fitted to the O_2 binding (see Methods).

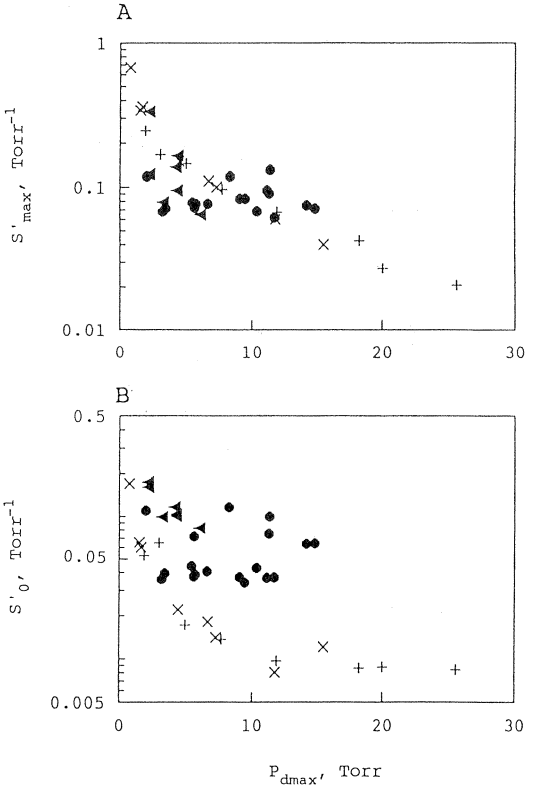

FIG. 5. S'_{max} and S'_0 values plotted as functions of P_{dmax}. (plus) Human Hb, (cross) Panulirus Hc, (closed triangle) *Tachypleus* Hc and (closed circle) *Limulus* Hc. The values were calculated on the basis of the fitted mathematical models (see Methods). The plots for human Hb were calculated on the basis of the Adair equation presented by Imai [5].

not observed between the S'_{max} and S'_0.

DISCUSSION

The results shown in Figure 4 show that the function dS/dP is generally maximized at P lower than that giving the maximum slope of the Hill plot ($P_{dmax} < P_{nmax}$). This means that the O_2 transport efficiency is maximized at P lower than that expected from the magnitude of the cooperativity. This was also true for human Hb [6], though some differences were observed in their relative magnitudes. In Hb the relationship $P_{dmax} < P_{50} < P_{nmax}$ was found for all the cases examined [6], but lobster (*Panulirus* and *Procambarus*) Hcs gave the relationship $P_{dmax} < P_{50} \simeq P_{nmax}$, whereas horseshoe crab (*Limulus* and *Tachypleus*) Hcs gave the relationship $P_{dmax} \leq P_{50} < P_{nmax}$.

In *Procambarus* Hc the Hill coefficient (n) for the 12-mer is significantly higher than that for the 6-mer [10], but in this study no significant difference was found in the S' *vs.* P plot. Apparently, the association to 12-meric structure seems to have little effect on the O_2 transport efficiency. It will be of interest to examine further the S' profiles of other 12-meric and 24-meric Hcs such as those of crabs and spiders.

The results of the present study show that the lobster Hcs resemble human Hb in a sense that the S' *vs.* P curves give a single and relatively symmetric peak, and also that the S'_0 values are relatively low. On the other hand, curves for the horseshoe crab Hcs are characterized by multiple peaks or shoulders tailing toward the low P region (Fig. 3B). In addition, in the case of *Limulus* Hc, the maximum transport efficiency, S'_{max}, was independent of P_{dmax}, while the S'_0 values were relatively high irrespectively of P_{dmax} (Fig. 5). The present results indicate that distinct differences exist between the lobster and horseshoe crab Hcs in the O_2 binding profile, which may be ascribed to the difference in the cooperativity mechanism.

The $S'0$ values for horseshoe crab Hcs were generally higher than those for lobster Hcs and Hb (Fig. 5B). This is because horseshoe crab Hcs bind O_2 almost non-cooperatively when P is low; previous studies [3, 8] have shown that the slope of Hill plot remains close to unity even up to $S=0.3$ in many cases examined. Therefore in the low P range the profile of the S' *vs.* P plot is analogous to that of Mb (Fig. 1), and the S' value increases rapidly as P approaches to 0, as exemplified in the diagram for *Tachypleus* Hc (Fig. 3B). In terms of the allosteric model this property is explained by a relatively low ratio of K_R/K_T and a large allosteric constant (L) [3, 8]. The protein molecule is confined in the state T at low P, and relatively a high P value is required for the allosteric transition to take place.

According to Brouwer and Serigstad [3], the O_2 binding to *Limulus* Hc can be described by the ICU model. In this model it is assumed that an equilibrium exists between the functional 6-mer and 12-mer, which undergo different allosteric transitions ($T_6 \leftrightarrow R_6$ and $T_{12} \leftrightarrow R_{12}$). By numerical examination of the model it was found that P values giving the maxima and shoulders in the S' *vs.* P curve correspond to those at which the T/R transitions take place in the functional 6-mer and 12-mer (data not shown). If the two switchover points are close in position, then maxima may apparently fuse into a single peak. Thus in the framework of the ICU model, the uniqueness of horseshoe crab Hc is explained by the presence of different functional species that make different allosteric transitions. More generally, the heterogeneity in the S' profile of horseshoe crab Hcs possibly arises from the huge molecular construction which allows many kinds of cooperative interactions. In the case of *Tachypleus* Hc, only a single peak was observed in the S' *vs.* P diagram under the conditions examined (Fig. 3B), and its O_2 equilibra could be fitted by the two-state model with m as an adjustable parameter (Eq. 4) [8].

Apart from such an allosteric model, it is also possible that in the horseshoe crab Hcs the subunit heterogeneity contributes to the functional heterogeneity. Horseshoe crab Hcs are composed of 6 or more different subunits, of which O_2 affinities differ by several folds [2, 9, 16], and this also can cause the heterogeneity in the O_2 binding.

In the O_2 carriers including vertebrate Hb and arthropod Hcs, it seems to be a general rule that they are most adapted to O_2 concentration lower than normal. This means that they are designed to function best in hypoxia, such as occurring under vigorous exercise. Particularly in arthropods, blood O_2 levels are strongly dependent on ventilatory and circulatory states [17], and the O_2 affinity of arthropod Hcs is modulated by various inorganic and organic ions such as H^+, Ca^{2+}, lactate and urate ions [17]. In crustacean Hcs, the O_2 affinity is increased by lactate, which is accumulated in the hemolymph under hypoxia or after physical exercise. Horseshoe crab Hcs lack such a lactate sensitivity, but this is covered by a large reverse Bohr effect [11]. At the lower end of the physiological pH, however, the reverse Bohr effect diminishes, and under severe hypoxic conditions the effect can not increase the O_2 affinity enough to meet the O_2 requirement [4]. The results of the present study show that the horseshoe crab Hcs still maintain a high O_2 transport efficiency in a wide range of P, particularly at a low P, independently of the functional modulators. This seems to be a new way of adaptation to ambient hypoxia and may be unique to O_2 carriers having large molecular constructions such as those found in horseshoe crab Hcs. It would be therefore interesting and worthwhile to examine the O_2 transport efficiency of other carriers in relation to their physiological function and mechanism of the cooperativity.

ACKNOWLEDGMENTS

The authors wish to thank Dr. S. Akiyama (Niigata University) for many helpful comments.

REFERENCES

1 Arisaka F, Van Holde KE (1979) Allosteric properties and the

association eqilibria of hemocyanin from *Callianassa californiensis*. J Mol Biol 134: 143–173

2 Brenowitz M, Bonaventura C, Bonaventura J (1984) Self-association and oxygen-binding characteristics of the isolated subunits of *Limulus polyphemus* hemocyanin. Arch Biochem Biophys 230: 238–249

3 Brouwer M, Serigstad B (1989) Allosteric control in *Limulus polyphemus* hemocyanin: functional relevance of interactions between hexamers. Biochemistry 28: 8819–8827

4 Diefenbach CO, Mangum CP (1983) The effects of inorganic ions and acclimation salinity on oxygen binding of the hemocyanin of the horseshoe crab, *Limulus polyphemus*. Mol Physiol 4: 197–206

5 Imai K (1979) Thermodynamic aspects of the co-operativity in four-step oxygen equilibrium of haemoglobin. J Mol Biol 133: 233–247

6 Kobayashi M, Ishigaki K, Kobayashi M, Imai K (1994) Shape of the haemoglobin-oxygen equilibrium curve and oxygen transport efficiency. Respir Physiol 95: 321–328

7 Makino N (1986) Analysis of oxygen binding of *Panulirus japonicus* hemocyanin. The effect of divalent cations on the allosteric transition. Eur J Biochem 154: 49–55

8 Makino N (1989) Hemocyanin from *Tachypleus gigas*, I. Oxygen-binding properties. J Biochem 106: 418–422

9 Makino N (1989) Hemocyanin from *Tachypleus gigas*. II. Cooperative interactions of the subunits. J Biochem 106: 423–429

10 Makino N, Ohnaka H (1991) Subunits and cooperativity of *Procambarus clarkii* hemocyanin. In Structure and Function of Invertebrate Oxygen Carriers Ed by SN Vinogradov, OH Kapp, Springer-Verlag, New York, pp. 99–107

11 Mangum CP (1983) The effect of hypoxia on hemocyanin-oxygen binding in the horseshoe crab *Limulus polyphemus*. Mol Physiol 3: 217–224

12 Minton AP, Imai K (1974) The three-state model: a minimal allosteric description of homotropic and heterotropic effects in the binding of ligands to hemoglobin. Proc Natl Acad Sci USA 71: 1418–1421

13 Monod J, Wyman J, Changeux JP (1965) On the nature of allosteric transition: A plausible model. J Mol Biol 12: 88–118

14 Richey B, Decker H, Gill SJ (1985) Binding of oxygen and carbon monoxide to arthropod hemocyanin: an allosteric analysis. Biochemistry 24: 109–117

15 Robert C H, Decker H, Richey B, Gill SJ, Wyman J (1987) Nesting: hierarchies of allosteric interactions. Proc Natl Acad Sci USA 84: 1891–1895

16 Sullivan B, Bonaventuna J, Bonaventura C(1974) Functional differences in the multiple hemocyanins of the horseshoe crab, *Limulus polyphemus* L. Pro Natl Acad Sci USA 71: 2558–2562

17 Truchot J P (1992) Respiratory function of arthropod hemocyanins. Adv Comp Env Physiol 13: 377–410

18 Wyman J (1964) Linked functions and reciprocal effects in hemoglobin: a second look. Adv Protein Chem 19: 223–286